



Calibration and Direct Georeferencing Analysis of a Multi-Sensor System for Cultural Heritage Recording

DAVID HERNÁNDEZ-LÓPEZ, MIRIAM CABRELLES, BEATRIZ FELIPE-GARCÍA & JOSÉ LUIS LERMA, Albacete, Valencia, Spain

Keywords: Multi-sensor system, calibration, orientation, cultural heritage

Summary: A large amount of cultural heritage monuments and sites exist distributed worldwide that require easy to use, cheap and fast sensor orientation tools for recording, georeferencing, surveying and mapping. Ground control points are usually required on site for close range photogrammetry to achieve accurate surveys, limiting both the involvement of non-experts and the chance to know the right place of the monuments unless a ground reference system is considered. This paper presents the system calibration of an image-based multi-sensor system that integrates two consumer-grade cameras, one global navigation satellite system (GNSS) and one low-cost inertial system, i.e., a micro-electro-mechanical system (MEMS) based inertial measurement unit (IMU). The multi-sensor system is calibrated indoor regarding both the camera orientation parameters and the boresight (rotations and offsets) parameters of the two digital cameras. The boresight parameters will be used to correct the direct approach estimates. The performance of the system calibration is tested outdoor on an upside down pyramidal sculpture to deliver both accurate 3D points and high resolution 3D models. Both scenarios are considered free of magnetic anomalies. The results achieved with the GNSS/MEMS-IMU direct approach are compared with the indirect approach based on bundle block adjustment. Further extrapolations to object space through digital surface models are also determined. The testing of the system shows that GNSS/MEMS-IMU data are good enough to provide approximate exterior orientation parameters of the cameras but not to yield accurate 3D models (<1–2 cm) for cultural heritage applications.

Zusammenfassung: *Kalibrierung und Analyse der direkten Georeferenzierung eines Multisensorsystems zur Aufnahme von Kulturdenkmälern.* Weltweit gibt es eine große Zahl an Denkmälern, die

zum Kulturerbe zählen und für deren Aufnahme, Vermessung und Kartierung einfach handhabbare, preiswerte und schnelle Sensor-Orientierungswerkzeuge benötigt werden. Für eine genaue Vermessung durch Nahbereichsphotogrammetrie werden vor Ort Passpunkte benötigt, was die Einbeziehung von Nichtexperten, aber auch die absolute Positionierung eines Denkmals ohne zusätzliche Information über das Referenzsystem behindert. Dieser Beitrag präsentiert die Kalibrierung eines Multisensorsystems, welches zwei übliche digitale Kameras, einen Empfänger für ein globales Satelliten-Navigationssystem (GNSS) und eine kostengünstige inertielle Messeinheit (IMU) auf Basis von mikroelektromechanischen Systemen (MEMS) integriert. Dieses Multisensorsystem wird im Labor sowohl hinsichtlich der Orientierungsparameter der Kameras als auch hinsichtlich deren Verschiebung und Verdrehung relativ zu den Positions- und Lagesensoren kalibriert. Die kalibrierten Werte dieser Verschiebungen und Verdrehungen werden bei der direkten Georeferenzierung zur Korrektur der durch diese Sensoren bestimmten Position und Lage des Systems verwendet. Die Güte dieser Systemkalibrierung zur Gewinnung von genauen 3D Punkten und hochaufgelösten 3D Modellen wird außerhalb des Labors anhand einer auf dem Kopf stehenden pyramidenförmigen Skulptur untersucht. Beide Szenarien werden als frei von magnetischen Anomalien angesehen. Die Ergebnisse der direkten Georeferenzierung basierend auf den GNSS/MEMS-IMU Sensoren werden mit einer indirekten Methode unter Verwendung einer Bündelblockausgleichung verglichen und Extrapolationen im Objektraum durch digitale Oberflächenmodelle bestimmt. Die Untersuchung des Systems zeigt, dass die Daten der GNSS/MEMS-IMU Sensoren gut genug sind, um genäherte Parameter für die äußere Orientierung der Kameras zu liefern, aber noch nicht dafür ausreichen, sehr genaue 3D Modelle (<1–2 cm) für die Aufnahme von Kulturdenkmälern zu erreichen.

1 Introduction

There are many cultural heritage architectural and archaeological objects, monuments and sites around the world that need appropriate recording. Accurate recording is mandatory for decay analysis, reconstruction, and monitoring over time. Close range photogrammetry has long been used to record cultural heritage. The classical approach was making use of metric cameras, acquiring stereo-pairs and manual plotting. With the advent of digital photogrammetry, two-dimensional rectifications and ortho image generation became popular in architectural recording. In the last years, there is a trend to automate image-based solutions either with metric cameras or with amateur cameras based on robust hierarchical detection and matching of image features (HAOA & MAYER 2003, POLLEFEYS et al. 2004, REMONDINO & RESSL 2006). The determination of the exterior orientation parameters is a conventional requirement whenever dealing with image-based photogrammetric datasets. An ideal scenario would be to achieve them quickly and accurately without any need of direct measurements based on total stations, GNSS and rulers, among others. However, direct georeferencing in close range photogrammetry is not widespread despite of its benefits to avoid measuring coordinated targets (KIRCHHÖFER et al. 2010, 2011).

Direct georeferencing using integrated relative kinematic GNSS/inertial systems has been investigated for more than one decade to determine the reliability and accuracy of directly measured orientation parameters in operational photogrammetric airborne environments (CRAMER et al. 2000, MOSTAFA & SCHWARZ 2001) and terrestrial mobile mapping systems (EL-SHEIMY & SCHWARZ 1999, DA SILVA et al. 2003). SKALLOUD (2006) reviews the essential features, methods and approaches in direct georeferencing of airborne sensors. There is no doubt that highly sophisticated integrated GNSS/inertial systems can be used to overcome traditional issues in aerial triangulation such as block design, determination of approximate exterior orientation parameters, reduction of interactive editing, more reliable feature matching and truly automatic processing. Nevertheless, GNSS/inertial data integra-

tion and uncorrected errors in the overall system calibration including not only the bore-sight misalignment and the GNSS offsets but the imaging sensors are the limiting factors to achieve high accuracy estimates in object space (CRAMER 2001). The most crucial task is to select the right calibration parameters for the system calibration (CRAMER & STALLMANN 2002). An analysis of the stability of the misalignments is required to avoid significant changes in the rotations, GNSS offsets and camera calibration parameters (JACOBSEN 2000). Furthermore, stereoplottling as well as some automatic image matching methods for digital elevation model (DEM) generation may be affected by y parallaxes (YASTIKLI & JACOBSEN 2002, 2005).

There is an increased interest in the topic of low-cost inertial navigation especially for pedestrian positioning systems (FELIZ et al. 2009, CHEN et al. 2009) and human motion tracking (FRANK 2010, SABATINI 2011). Stand-alone MEMS trajectory determination is an actual challenge despite of the recent improvements in the performance of small and light-weight systems (WOODMAN 2007). Compared to high-end tactical and navigation IMUs, with MEMS-IMU it is difficult to determine an accurate heading due to the drift of low-cost MEMS gyroscopes and unpredictable perturbation of the magnetic field (CHEN et al. 2009). Recent scientific publications are tackling the latter effect mitigating the magnetic anomalies in environments such as urban canyons and indoor (AFZAL et al. 2011a, b, TOME & YALAK, 2008).

Low-cost multi-sensor systems for positioning can integrate a diverse set of devices such as a laptop, a consumer GNSS, a digital compass, a video camera (HAALA & BÖHM 2003), a MEMS inertial sensor, a webcam and a display system (PORTALÉS et al. 2010), a personal digital assistant (PDA) or a smartphone with integrated camera and MEMS based orientation and positioning sensors. The accuracy requirements for cultural heritage applications are nowadays neither fulfilled with consumer GNSS nor smartphone devices. The limiting factor is the theoretical positioning accuracy of the code-based GNSS, although its absolute accuracy can be improved after the system calibration due to the partial compensation of

the positional errors (KIRCHHÖFER et al. 2011). On the contrary, MEMS-IMU results integrated with differential GNSS (or better DGNSS) are promising for navigation-type applications such as mobile mapping systems (SCHWARZ & EL-SHEIMY 2004, GARCÍA-ASENJO et al. 2008, KIRCHHÖFER et al. 2010).

This paper aims at an analysis of the performance of the overall system calibration of an image-based multi-sensor system for architectural/archaeological recording under scenarios without disturbances of the magnetic field. The GNSS will be used to estimate the position, while the low-cost MEMS-IMU will be used for orientation determination. The data acquisition will follow a stop-and-go strategy. This system might be used to survey other scenarios such as outcrops in geomorphology, large civil engineering structures and 3D city models namely in opened areas, among others. In section 2 the geometric relationship between the GNSS, IMU and the two cameras is briefly reviewed and particularized for the image-based multi-sensor system with two consumer-grade cameras. In section 3 the overall system calibration results are described. In section 4 the performance of the direct georeferencing approach with GNSS/MEMS-IMU and the indirect approach with bundle block adjustment when modelling a large archaeological sculpture is analysed and discussed. A conclusion of the research carried out for cultural heritage recording is presented in section 5.

2 Geometric Relationship of the Sensors

The direct georeferencing model sets up the geometric relationship of a multi-sensor system, i.e., digital camera (*c*-frame), IMU body frame (*b*-frame) and the GNSS antenna in the ground coordinate system (*m*-frame). The relationship among the different sensors can be written as follows (1):

$$\begin{bmatrix} X \\ Y \\ Z \end{bmatrix}_m = \begin{bmatrix} X_{GNSS} \\ Y_{GNSS} \\ Z_{GNSS} \end{bmatrix}_m - R_b^m \begin{bmatrix} ax \\ ay \\ az \end{bmatrix}_b^{GNSS} + R_b^m \begin{bmatrix} dx \\ dy \\ dz \end{bmatrix}_c^b + \alpha R_b^m dR_c^b \begin{bmatrix} x \\ y \\ -f \end{bmatrix}_c \quad (1)$$

where X, Y, Z are ground coordinates, $X_{GNSS}, Y_{GNSS}, Z_{GNSS}$ are ground coordinates of the centre of phase of the GNSS antenna, ax, ay, az the offsets of the centre of phase of the GNSS antenna relative to the IMU centre (*b*-frame origin), R_b^m is the rotation matrix of the *b*-frame into the *m*-frame; dx, dy, dz are the offsets of the projection centre relative to the IMU centre; α is a scale factor; dR_c^b is the rotation matrix of boresight misalignment; x, y are the image coordinates; and finally f the principal distance.

Our multi-sensor system integrates two digital cameras, one virtual reference station (VRS)-GNSS rover receiver, one low-cost MEMS-IMU, and a laptop for operating, synchronizing and saving the data coming from the sensors. All the sensors are attached to a portable pitch and yaw rotating mount (Fig. 1a). This portable two axis multi-sensor rotating mount is an evolution of a previously designed 1 axis rotating mount (LERMA et al. 2010) that allows free image data acquisition without losing the satellite signals when shooting upwards or downwards the horizontal plane. Thus, this mount minimises the problem of antenna tilt and loss of signal or multipath effects when large pitch angles are required for recording.

The devices selected for the project presented herein are two single lens reflex (SLR) digital cameras, one Canon EOS 1Ds Mark III (21.9 MPixels) with a Canon EF 24 mm F2.8 and another low resolution camera Canon EOS D60 (6.3 MPixels) with a Sigma 15–30 mm F3.5–4.5 EX DG Aspherical (fixed at 15 mm and focused at infinity). A summary of the camera specifications is presented in Tab. 1. An Xsens MTx inertial system (Tab. 2) is used to provide the attitude information of the multi-sensor system. From the specifications, it is understood that the MEMS-IMU

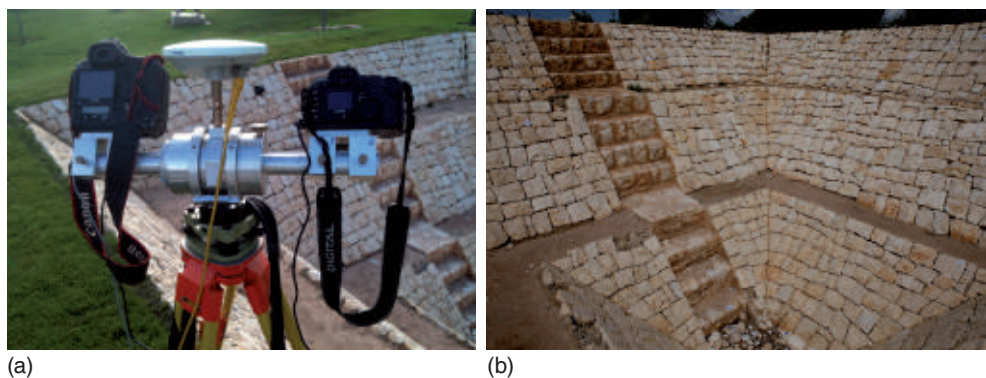


Fig. 1: (a) Close-up view of the image-based multi-sensor system, (b) outdoor testfield.

Tab. 1: Camera specifications.

Camera	Canon EOS 1Ds Mark III	Canon EOS D60
Resolution (pixel)	5616 x 3744	3072 x 2048
Sensor size (mm)	36 x 24	22.7 x 15.1
Pixel size (μm)	6.4	7.4
Sensor size	Full frame (36 mm x 24 mm)	APS-C (22.7 mm x 15.1 mm)
Focal length (mm)	24	15 (24 full frame equivalent)
Image quality	RAW	RAW
Lens	Canon EF 24 mm F2.8	Sigma 15–30 mm F3.5–4.5 EX DG

Tab. 2: Xsens MTx specifications.

Angular Resolution	0.05 deg
Static Accuracy (Roll/Pitch)	< 0.5 deg
Static Accuracy (Heading)	< 1 deg
Dynamic Accuracy	2 deg RMS
Maximum update rate onboard	120 Hz

static accuracy in roll and pitch is <0.5 deg and in yaw <1 deg (in homogeneous magnetic environment). A proprietary Xsens MTx sensor fusion algorithm to combine magnetometer and gyroscope data was used to orient the device relative to the global reference frame. The inertial sensor is placed inside the housing of the portable mount nearby the centre of rotation; the Trimble Zephyr antenna is fitted on top of the mount. A Trimble 5700 GPS receiver in VRS mode is used to determine the coordinates of the antenna phase centre. The expected positioning accuracy is approxi-

mately 2–3 cm (RETSCHER 2002). The accuracy depends on the number of collected data between the rover and the receiver to fix signal ambiguity with integers. When the ambiguity can not be fixed with integers, a float solution can be calculated that degrades the solution to a decimetre level (EL-RABBANY 2002). Fig. 1 shows the image-based multi-sensor system at the Polytechnic University of Valencia testfield. The image-based multi-sensor system presented herein differs from those published by LERMA et al. (2010) and KIRCHHÖFER et al. (2011). The former only has got a free yaw-angle rotation while the latter integrates only one digital SLR camera.

The idea of integrating two cameras on the mount is five-fold: first, to improve reliability in the data acquisition (the simultaneous acquisition of two images avoids troubles in case of unexpected camera errors on site); second, it allows multiband image acquisition when requested, for instance, for building inspections with two cameras, one visible and

another thermal (such as in the solution presented by ALBA et al. 2011 and LERMA et al. 2010); third, it facilitates image fusion due to the rigid body transformation between cameras; fourth, it eases the comparison and the extrapolation of output results; and fifth, the multi-sensor system might work as a stereoscopic system with an appropriate base and camera-object distance ratio. In this paper, the cameras are not supposed to work as stereopairs from each station but as a multi-acquisition system acquiring data from multiple stations.

3 Overall System Calibration

The overall system calibration is required to relate GNSS-derived positions, IMU-derived attitude parameters and imagery-derived attitude parameters. Fig. 2 shows the frame of the multi-sensor system without the GNSS-antenna and cameras; only the MEMS-IMU is inside the metal frame. Next, the indoor approach for calibrating the system is presented.

The system calibration was undertaken in a static close range fashion following three main steps:

1. camera calibration of the two cameras,
2. determination of the origin of the IMU placed inside the mount and some auxiliary marks, and
3. boresight calibration among the sensors.

For the first step, two self-calibration bundle adjustments were independently carried out, one for each camera, to determine the interior orientation parameters (for details, see CABRELLES 2010). To achieve high precision in the camera calibration parameters, an optimised object space full of well-distributed targets and a convergent image space configuration was conducted to strengthen the overall network geometry and the camera station configuration (REMONDINO & FRASER 2006). The indoor testfield full of coded targets used to calibrate the multi-sensor system is presented in Fig. 2.

The familiar eight-parameter model with principal distance, principal offset and corrections for radial and decentering distortion was selected to estimate the interior orientation parameters. The adjustment included 9 images for the Canon EOS 1Ds Mark III and 8 for the Canon EOS D60. The output interior orientation parameters for the two cameras are presented in Tab. 3. All the parameters were significant for the former camera; for the latter, radial distortion parameter K3 and decentering distortion parameter P1 proved insignificant and were removed by the self-calibration approach. The standard deviations were always better by one order of magnitude for the 1Ds Mark III than for the D60.

It is essential to model radial lens distortion to effectively achieve high accuracy, especially for consumer-grade digital cameras (CHAN-

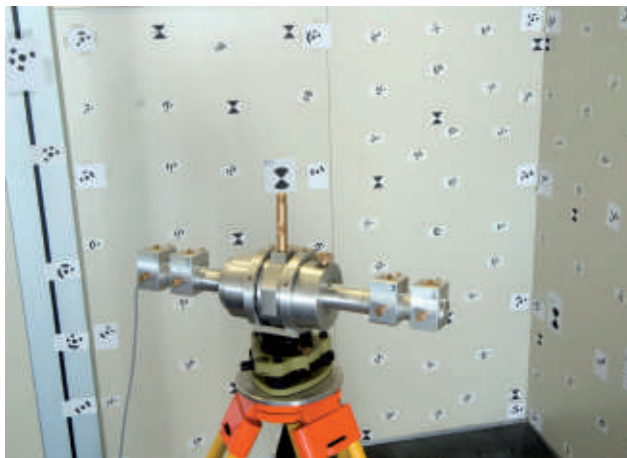


Fig. 2: Indoor testfield used to calibrate the multi-sensor system.

Tab. 3: Interior orientation parameters achieved for the two cameras and related standard deviations.

Parameters	Canon EOS 1Ds Mark III		Canon EOS D60	
	Value	Standard deviation	Value	Standard deviation
f (pixel)	-3819.93	0.03	-2099.53	0.19
x_0 (pixel)	-26.47	0.03	12.26	0.12
y_0 (pixel)	25.53	0.04	-17.79	0.31
K_1 (pixel ⁻²)	7.57E-09	5.29E-12	1.99E-08	8.30E-11
K_2 (pixel ⁻⁴)	-4.60E-16	1.03E-18	-1.98E-15	2.64E-17
K_3 (pixel ⁻⁶)	-3.42E-24	6.10E-26		
P_1 (pixel ⁻¹)	6.33E-08	6.63E-10		
P_2 (pixel ⁻¹)	3.15E-08	8.87E-10	2.01E-07	2.15E-08

DLER et al. 2005, WACKROW et al. 2007, WACKROW & CHANDLER 2008).

The second step of the overall system calibration started with the determination of the origin of the IMU that is placed inside the mount. The multi-sensor system was dismantled and only the central metallic bar hosted the attached IMU as well as the four screws used to attach the two camera mounts. The four screws were used as auxiliary marks to relate the origin of the IMU and the position of the camera centres once the mount is assembled. The bar was photographed from multiple images and the marks measured on the images. A bundle block adjustment was undertaken to determine the spatial offsets between the origin of the IMU b -frame and the centres of the four screws (screws 1, 2 for the Canon EOS 1Ds Mark III and screws 3, 4 for the Canon EOS D60, Fig. 3).

The third and last step in the overall system calibration was the determination of the boresight parameters between the sensors: the IMU, the two cameras and the GNSS antenna. For this third step, the assembled multi-sensor system mount was carefully levelled and oriented parallel to the object space coordinate system to transform the raw IMU angles into the m -frame. The orientation parallel to the object space coordinates was required to transform the raw IMU κ reading (which refers to a global coordinate frame) to its equivalent in the local coordinate system that was used for calibration. Several images were taken with the Canon EOS 1Ds Mark III to determine:

a) the centre of the GNSS screw; b) the centres of the four screws. Afterwards, the two SLR cameras were attached to the multi-sensor system mount and two images were taken, one with each camera, to determine the perspective centres and the rotations. The centre of the GNSS screw was modified to account for the shift between the base of the GNSS antenna and its centre of phase. This latter value was provided by the GNSS manufacturer and added to compute the GNSS offset between the GNSS antenna and the IMU b -frame, i.e., ax , ay and az in (1). The centres of the screws in b) were used as auxiliary marks to determine the camera-IMU offset parameters dx , dy and dz (1) owing to the position of the MEMS-IMU inside the chase. This was possible because the system was not moved when the cameras were attached to their mounts, so that the positions of the screws in the object coordinate system did not change in this process. A final bundle adjustment with all the images acquired in this step was carried out to determine the boresight parameters. The differences between the IMU rotation angles and the bundle adjustment orientation angles yielded the boresight misalignment (dR_c^b). Tabs. 4 and 5 summarise the offsets and the boresight misalignments of the multi-sensor system, respectively, considering the IMU b -frame as the origin, Fig. 3. FOTOGIFLE photogrammetric software (developed in-house by the authors) was used to determine the estimates of the overall system calibration.

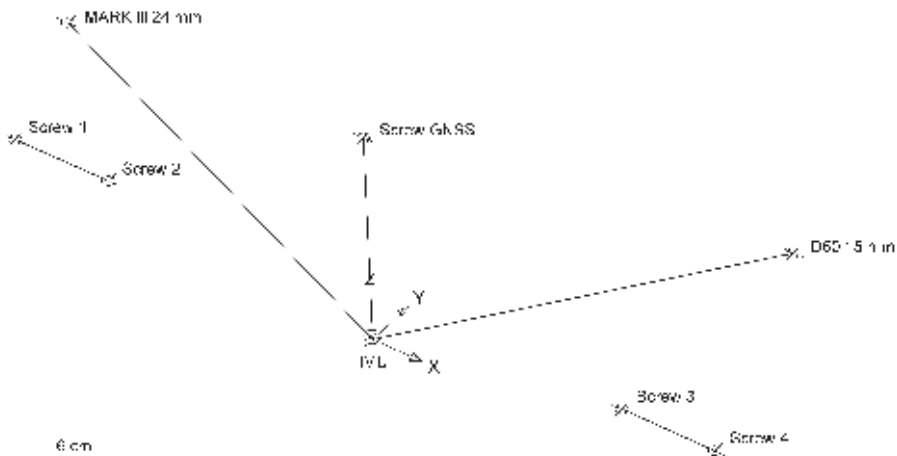


Fig. 3: Offsets among the camera perspective centres (Canon EOS 1Ds Mark III and Canon EOS D60), the centre of the screw of the GNSS antenna and the origin of the IMU; screws 1 up to 4 are used as auxiliary marks for the two cameras.

Tab. 4: Offsets and standard deviations after the overall system calibration.

Point	X (mm)	Y (mm)	Z (mm)	σ_x (mm)	σ_y (mm)	σ_z (mm)
IMU	0.0	0.0	0.0	< 0.1	0.1	< 0.1
Centre 1Ds Mark III	-199.1	11.6	114.1	0.1	0.1	< 0.1
Centre D60	193.9	109.4	71.9	0.4	0.1	0.3
Screw GNSS	-3.4	4.3	131.9	< 0.1	0.1	0.1

Tab. 5: Boresight misalignments and standard deviations after the overall system calibration.

Camera	$\Delta\omega$ (g)	$\Delta\phi$ (g)	$\Delta\kappa$ (g)	σ_ω (g)	σ_ϕ (g)	σ_κ (g)
Canon EOS 1Ds Mark III	1.3221	0.8161	-0.3252	0.0012	0.0012	0.0016
Canon EOS D60	-0.0952	0.6256	-1.0179	0.0074	0.0023	0.0093

As it can be checked in Tab. 4, the results of the overall system calibration on the indoor testfield are better than 0.2 mm (1σ); only the perspective centre of the Canon EOS D60 yields standard deviation up to 0.4 mm in the X axis and 0.3 mm in the Z axis. Tab. 5 summarises the boresight misalignments between the bundle adjustment and the transformed IMU attitudes into ω , ϕ and κ . The corresponding standard deviations determined in the bundle adjustment solution are up to 6.2, 1.9 and 5.8 times larger for the Canon EOS D60.

4 Performance of Direct Georeferencing

The performance of direct georeferencing has been investigated on an upside-down pyramidal sculpture on the campus of the Polytechnic University of Valencia (Fig. 1b). This sculpture is considered as an excellent testfield due to its complex geometry full of texture for the image measurements. A total of suitable 36 coded-target ground control points were surveyed by a Topcon IS Total Station; the accuracy of signalled control points is better than 0.005 m. Four ground control

points nearby the sculpture were used before and after the measurements to set up the relationship between the local coordinate system and the european terrestrial reference system 1989 (ETRS89). A systematic shift of -0.025 m , -0.044 m and -0.120 m was found in the VRS-GNSS coordinates making use of the ERVA network (ERVA 2012).

As reported by WACKROW & CHANDLER (2008), a mildly convergent camera configuration can be used to minimise eventual systematic error surfaces caused by slightly inaccurate lens distortion parameters for DEM generation. Herein, a stop-and-go sequential acquisition mode at intervals of roughly 60 s at 8 stations following a strip with convergent axes at both extremes was carried out to verify the quality of the overall system calibration. Fig. 4 displays the 8 stations represented by the 16 camera positions.

An indirect approach was used to derive the exterior orientation parameters for each recorded image in a bundle adjustment integrating both cameras. A maximum root-mean-square error (RMSE) of 3 mm was achieved in object space on the ground control points. All the coded-target measurements in image-space were measured automatically with subpixel accuracy in PhotoModeler 6.0. The tie points between consecutive images corresponding to the two cameras were measured manually. All the points used in the bundle block adjustment (BBA) together with the exterior orientation of the cameras are displayed in Fig. 4.

To assess the differences of the direct georeferencing approach and the photogrammetric image-based approach from multiple stations, the raw roll, pitch and yaw angles determined by the MEMS-IMU were converted into ω , ϕ and κ . The magnetic declination was considered to refer the κ angle to the geodetic north (GARCÍA-ASENJO et al. 2008). The rotation matrix was corrected with the boresight misalignment parameters before transforming with two rigid body transformations (one for each camera) the GNSS coordinates measured at the antenna phase centre into the theoretical projection centres of the cameras. The mathematical routines were developed by the authors. In Figs. 5 and 6 the particular attitude and position differences after the overall system calibration carried out indoors are shown for the distinct camera stations taken on site around the sculpture. In other words, Figs. 5 and 6 present the residuals (differences) of the boresight misalignments and the GNSS offsets for the two cameras, respectively.

The differences of the boresight misalignments (Fig. 5) are quite consistent with zero mean for the three rotation angles in both cameras. The RMSEs for the Canon EOS 1Ds Mark III are 0.0136 gon in ω and ϕ , and more than one order of magnitude higher in κ , 0.1470 gon; for the Canon EOS D60 slightly worse, 0.0206 gon in ω , 0.0187 gon in ϕ and 0.1496 gon in κ . In both cameras, the instability of κ compared with ω and ϕ is apparent. It should be noted that the RMSEs for the three rotations are smaller than the RMSEs

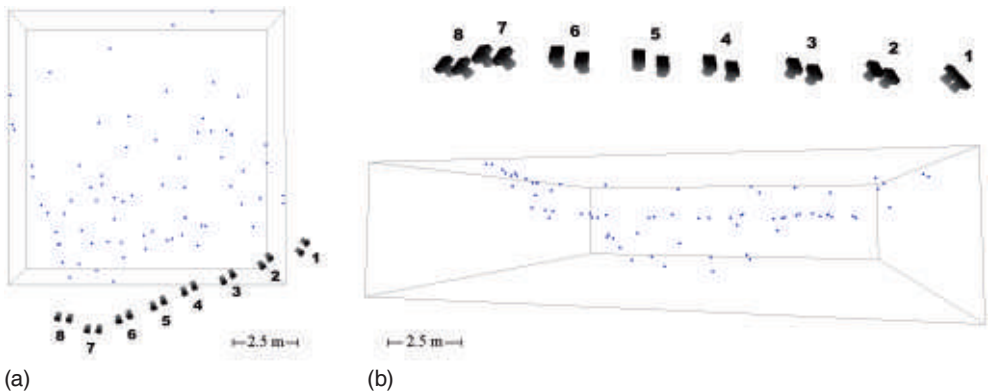


Fig. 4: Two perspective views of the strip 8 stop-and-go stations, (a) top view, (b) front view. The blue dots are the tie points and the ground control points measured for the BBA.

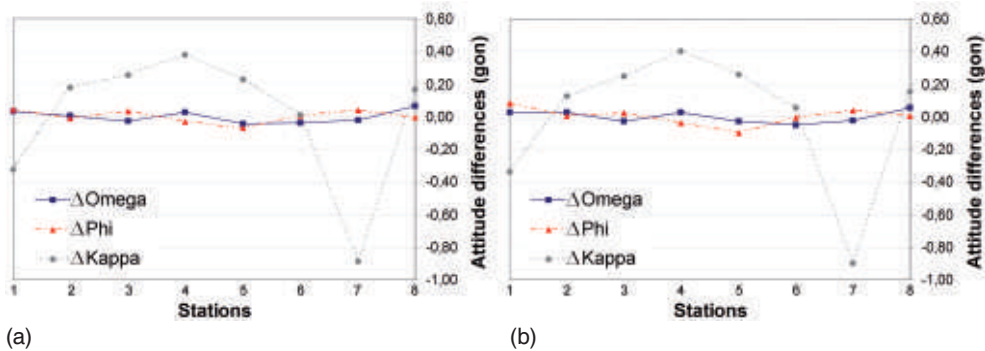


Fig. 5: Comparison of attitudes from reference bundle block adjustment and MEMS-IMU on site: (a) Canon EOS 1Ds Mark III, (b) Canon EOS D60.

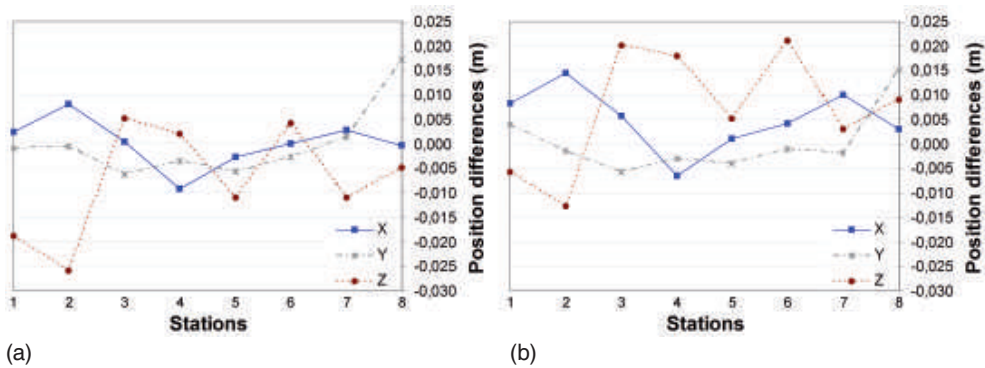


Fig. 6: Comparison of projection centres from reference bundle block adjustment and GNSS on site: (a) Canon EOS 1Ds Mark III, (b) Canon EOS D60.

of the attitudes provided by the manufacturer (Tab. 2).

Analysing the differences of the GNSS offsets after calibration presented in Fig. 6, the results for the Canon EOS 1Ds Mark III yield a zero mean in planimetry, and -7 mm in Z. However, for the Canon EOS D60, there is a mean value for the offsets of 5 mm in X, 0 mm in Y and 7 mm in Z, with RMSE values of 2 mm in X, 2 mm in Y and 4 mm in Z. The RMSEs for the Canon EOS 1Ds Mark III are 2 mm, 3 mm and 4 mm in X, Y and Z, respectively. It is worth mentioning that the departure from the mean of the height in both cameras points in opposite directions. To a lesser extent, the X-axis is also pointing in opposite directions due to the lack of accuracy of the angle κ of the MEMS-IMU. The achieved positioning accuracy is within the limits of the GNSS.

Based on the exterior orientation determined by the direct and indirect approaches, object coordinates of measured image points were computed by combined intersection independently for the two cameras. The combined spatial intersection corresponds to a bundle adjustment without control points, using the exterior orientation as fixed values and all available observations in the different images for the ground point measurement (YASTIKLI & JACOBSEN 2005).

The results presented in Fig. 7a show the mean differences in X, Y and Z considering as ground truth the six check points measured by the image total station for both the direct and the indirect approaches with the two cameras independently; Fig. 7b concentrates on the corresponding RMSEs. On the one hand, the quality of the indirect approach with bundle adjustment is similar for both cameras despite

their specifications (Tab. 1). The mean differences in position are in the range of 1 mm and 2 mm, and RMSEs up to 3 mm in Y for the Canon EOS D60. On the other hand, the direct approach yields both larger differences and larger RMSEs. The mean differences are approximately 1 cm (Fig. 7a). However, the RMSEs up to 4 cm are larger for the Canon D60 (approx. 1.4 times for the three components). Without any doubt, the uncertainty of the VRS-GNSS in positioning (with RMSEs not better than 1–2 cm) is a limiting factor to improve the quality of the output coordinates. A review of the accuracy performance of VRS networks can be found in RETSCHER (2002).

As expressed in JACOBSEN (2000), the absolute accuracy is only one result. The relative accuracy represented by the y parallax is important for the model setup, especially for the stereoscopic view. In addition, it might affect the performance of image matching. Tab. 6 presents the y parallax achieved after bundle block adjustment and direct georeferencing. The difference in quality is significant, below 1/3 of a pixel for bundle adjustment with maximum parallaxes below 1.5 pixels and higher for the direct referencing approach. The RMSE of y parallax is in the range of 4 pixels

for the Canon EOS D60 and almost 8 pixels for the Canon EOS 1Ds Mark III are both unacceptable for stereo-plotting; the maximum y parallaxes go up to 19.7 and 34.2 pixels, respectively. The larger errors in the Canon EOS 1Ds Mark III digital camera are owing to its higher resolution. In fact, the y parallax values for the Canon EOS 1Ds Mark III are slightly below the height resolution ratio (that equals 1.82).

Regarding derived XYZ coordinates in object space, despite of the mean differences (Fig. 7a) being within the accepted tolerance in large architectural documentation projects with typical mapping scales of 1:100 or 1:200, the large RMSEs can yield computations with large deviation errors (up to 10 cm). This fact is clearly visible when extrapolating the exterior orientation parameters to dense image matching, e.g. for 3D modelling. A statistical analysis shows the metric differences on the digital surface models for the two different solutions, direct referencing and indirect referencing (Fig. 8). 43.2% of the digital surface model is in the range of 0 and –2 cm, with maximum differences up to 2 cm (24.9%) and –10 cm (29.3%). These results coming from direct referencing allow us to confirm that the

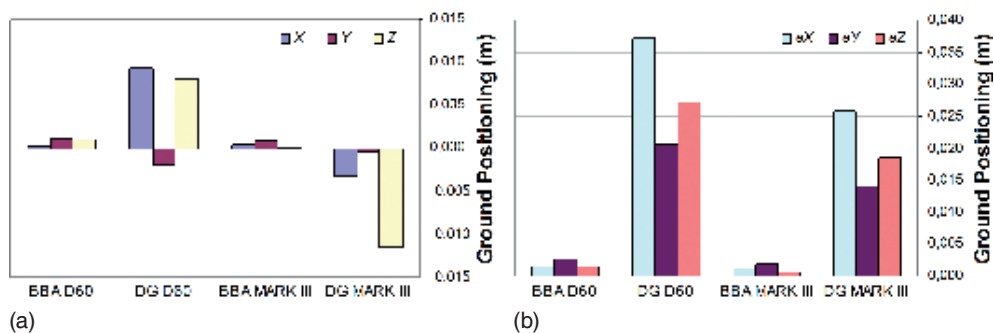


Fig. 7: (a) Mean differences and (b) RMSEs at the check points considering blocks with 8 images after bundle block adjustment (BBA) and direct georeferencing (DG).

Tab. 6: RMS y parallax errors of the blocks.

Approach	Number of images	Number of check points	RMSE of y parallax (pixel)	Max. y parallax (pixel)
BBA Canon EOS D60	8	55	0.3	1.5
DG Canon EOS D60	8	55	4.3	19.7
BBA Canon EOS 1Ds Mark III	8	61	0.3	1.3
DG Canon EOS 1Ds Mark III	8	61	7.6	34.2

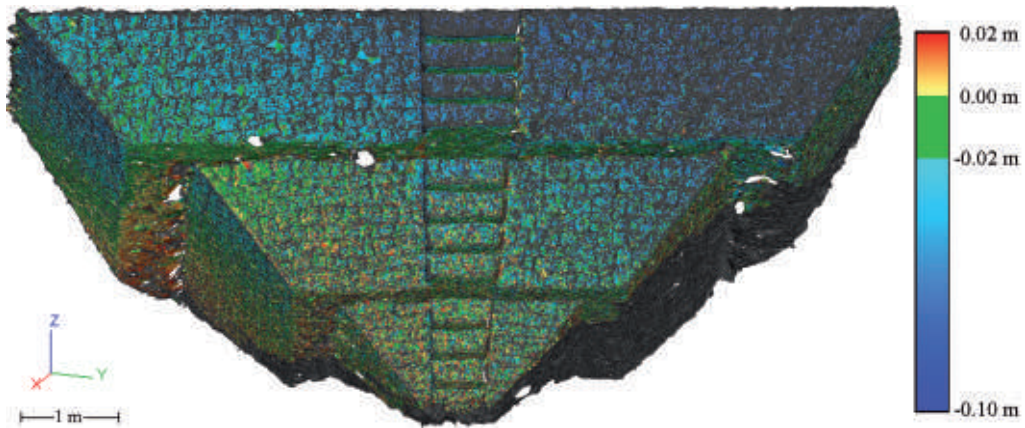


Fig. 8: Comparison of the digital surface models coming from direct and indirect georeferencing.

estimates are good as initial estimation for the exterior orientation problem and visualisation but not good enough to achieve accurate 3D models in close range applications following the presented methodology.

Three main factors affect the estimates of both relative and absolute accuracy with direct georeferencing: first, the influence of a VRS-GNSS systematic shift namely in the Z axis; second, the IMU rotation errors namely in κ ; and third, the inherent errors due to the overall system calibration carried out indoor. Regarding the relative accuracy, the non-zero mean difference when positioning with the direct approach (particularly in Z upwards for one camera and downwards for the other, Fig. 6) affects directly the quality of the output results, not only in object space (Fig. 7) but also in the image space (Tab. 5). In addition to the previous statement, the rotation estimates determined by the MEMS-IMU with their corresponding errors also affect the outputs in object space, namely the XY due to the κ error (Fig. 7) and slightly in Z due to ω and ϕ rotation errors. From a photogrammetric point of view, one way to improve the overall accuracy will be to carry out a combined block adjustment (also known as integrated sensor orientation). Alternatively, a combination of global direct georeferencing and local indirect orientation approaches can also be considered as an optimised way to perform georeferencing on monuments and sites. The alternative approaches dealing with global and local ori-

entation approaches to improve the reliability of the georeferenced data will be presented in future papers. Nevertheless, the results presented in this paper yield better accuracy estimates than other recording solutions (DA SILVA et al. 2003, GARCÍA-ASENJO et al. 2008, KIRCHHÖFER et al. 2010, 2011), even without combined block adjustment. More tests are necessary to confirm the reliability of the presented recording system for cultural heritage documentation.

5 Conclusions

This paper addresses the indoor overall calibration of an image-based multi-sensor system that integrates two SLR digital cameras, a low cost MEMS-IMU and a VRS-GNSS. The overall calibration includes the determination of both the interior orientation parameters and the boresight parameters. Once calibrated, the system is ready to carry out photogrammetric surveys outdoor despite of its relative accuracy is not appropriate for stereoscopic viewing with VRS-GNSS/MEMS-IMU direct georeferencing. The results presented in this paper demonstrate that mean differences of 1 cm and RMSEs in the range of 2–3.5 cm can be achieved with an image-based multi-sensor system performing direct georeferencing both in orientation and in spatial intersection. The multi-sensor system can be used to integrate different imaging devices, for instance,

cameras with different focal lenses or cameras with different spectra such as visible and near infrared. Furthermore, the multi-sensor system can be used either as a conventional stereoscopic system from each station or as a stereoscopic solution from multiple stations based on direct georeferencing. Using cameras of similar specifications except resolution, a slight improvement in quality by a factor of 1.4 is possible when increasing the resolution of a SLR digital camera from 6.3 up to 21.9 MPixel. The influence of the overall system calibration is of paramount importance to achieve maximum accuracy in daily projects. The limiting factors in the error budget are the κ angle and the VRS-GNSS solution. The bundle adjustment approach delivers highly reliable results with strong network geometry and enough number of images. Nevertheless, the inner camera geometry has to be properly modeled. The presented results proved that the quality of direct exterior orientation measurements using VRS-GNSS/MEMS-IMU for medium accuracy (1–4 cm) heritage documentation projects is feasible; projects demanding more accuracy require different processing to improve the quality of the exterior orientation parameters. One way to improve the quality is to carry out a combined block adjustment (integrated sensor orientation) with at least one control point or preferably without ground control points.

Further research is required to confirm the feasibility of the presented image-based multi-sensor system in a variety of complex scenarios namely with GNSS shortages and with magnetic anomalies. For those circumstances, different indirect photogrammetric approaches will be used to bridge the gap to direct georeferencing.

Acknowledgements

The authors would like to thank for the support provided by the Spanish Ministry of Science and Innovation to the project HAR2010-18620. Special thanks need to be expressed to Dr. LUIS GARCÍA-ASENJO and Mr. PASCUAL GARRIGUES from the Polytechnic University of Valencia for their contributions.

References

- ALBA, M.I., BARAZZETTI, L., SCAIONI, M., ROSINA, E. & PREVITALI, M., 2011: Mapping Infrared Data on Terrestrial Laser Scanning 3D Models of Buildings. – *Remote Sensing* **3**: 1847–1870.
- AFZAL, M.H., RENAUDIN, V. & LACHAPPELLE, G., 2011a: Multi-Magnetometer Based Perturbation Mitigation for Indoor Orientation Estimation. – *Navigation* **58** (4): 279–292.
- AFZAL, M.H., RENAUDIN, V. & LACHAPPELLE, G., 2011b: Use of Earth's Magnetic Field for Mitigating Gyroscope Errors Regardless of Magnetic Perturbation. – *Sensors* **11** (12): 11390–11414.
- CABRELLES, M., 2010: Calibración geométrica de cámaras en dispositivos métricos y parametrización de sus descentrados ópticos. – Diploma Thesis, Universitat Politècnica de València.
- CHANDLER, J.H., FRYER, J.G. & JACK, A., 2005: Metric capabilities of low-cost digital cameras for close range surface measurement. – *The Photogrammetric Record* **20** (109): 12–26.
- CHEN, W., FU, Z., CHEN, R., CHEN, Y., ANDREI, O., KROGER, T. & WANG, J., 2009: An integrated GPS and multi-sensor pedestrian positioning system for 3D urban navigation. – 2009 Joint Urban Remote Sensing Event: 1–6, Shanghai.
- CRAMER, M., STALLMANN, D. & HAALA, N., 2000: Direct georeferencing using GPS/inertial exterior orientations for photogrammetric applications. – *The International Archives of the Photogrammetry, Remote Sensing and Spatial Information Sciences* **33** (B3): 198–205.
- CRAMER, M., 2001: Performance of GPS/inertial solutions in photogrammetry. – FRITSCH, D. & SPILLER, R. (eds.): *Photogrammetric Week 2001*: 49–62, Wichmann, Heidelberg, Germany.
- CRAMER, M. & STALLMANN, D., 2002: System calibration for direct georeferencing. – *The International Archives of Photogrammetry, Remote Sensing and Spatial Information Sciences* **34** (3A): 79–84.
- DA SILVA, J.F.C., CAMARGO, P.D.O. & GALLIS, R.B.A., 2003: Development of a low-cost mobile mapping system: a South American experience. – *The Photogrammetric Record* **18** (101): 5–26.
- EL-RABBANY, A., 2002: Introduction to GPS: the Global Positioning System. – Artech House, Boston, MA.
- EL-SHEIMY, N. & SCHWARZ, K.P., 1999: Navigating urban areas by VISAT – A mobile mapping system integrating GPS/INS/digital cameras for GIS applications. – *Navigation* **45** (4): 275–285.
- ERVA 2012: <<http://icverva.icv.gva.es:8080>> (2012-03-09).

- FELIZ, R., ZALAMA, E. & GÓMEZ GARCÍA-BERMEJO, J., 2009: Pedestrian tracking using inertial sensors. – *Journal of Physical Agents* **3** (1): 35–42.
- FRANK, K., VERA NADALES, J. & ANGERMANN, M., 2010: Reliable Real-Time Recognition of Motion-Related Human Activities Using MEMS Inertial Sensors. – ION GNSS 2010, Portland, Oregon, USA.
- GARCÍA-ASENJO, L., LERMA, J.L., GARRIGUES, P., BABELGA, S., CABRELLES, M., HERNÁNDEZ, D., BUCHÓN, F. & NAVARRO, S., 2008: Integración de GNSS y un sistema de navegación inercial de bajo coste para la georeferenciación directa de imágenes fotogramétricas. – *International Congress on Geomatic & Surveying Engineering*: 9 p., Valencia [on CD-ROM].
- HAALA, N. & BÖHM, J., 2003: A multi-sensor system for positioning in urban environments. – *ISPRS Journal of Photogrammetry & Remote Sensing* **58**: 31–42.
- HAOA, X. & MAYER, H., 2003: Orientation and auto-calibration of image triplets and sequences. – *The International Archives of the Photogrammetry, Remote Sensing and Spatial Information Sciences* **34** (3/W8): 73–78.
- JACOBSEN, K., 2000: Potential and limitation of direct sensor orientation. – *The International Archives of the Photogrammetry and Remote Sensing* **33** (B3/1): 429–435.
- KIRCHHÖFER, M.K., CHANDLER, J.H. & WACKROW, R., 2010: Testing and application of a low-cost photogrammetric recording system suitable for cultural heritage recording. – *Proceedings of RSP-Soc and Irish Earth Observation Symposium*: 330–337 [on CD-ROM].
- KIRCHHÖFER, M.K., CHANDLER, J.H. & WACKROW, R., 2011: Cultural heritage recording utilising low-cost close-range photogrammetry. – *Proceedings of CIPA 23rd International Symposium*: 8 p., Prague, Czech Republic [on CD-ROM].
- LERMA, J.L., NAVARRO, S., CABRELLES, M. & SEGUÍ, A.E., 2010: Camera calibration with baseline distance constraints. – *The Photogrammetric Record* **25** (130): 140–158.
- MOSTAFA, M.M.R. & SCHWARZ, K.P., 2001: Digital image georeferencing from a multiple camera system by GPS/INS. – *ISPRS Journal of Photogrammetry & Remote Sensing* **56**: 1–12.
- POLLEFEYS, M., VAN GOOL, L., VERGAUWEN, M., VERBIEST, F., CORNELIS, K. & TOPS, J., 2004: Visual Modeling with a Hand-Held Camera. – *International Journal of Computer Vision* **59** (3): 207–232.
- PORTALÉS, C., LERMA, J.L. & NAVARRO, S., 2010: Augmented reality and photogrammetry: A synergy to visualize physical and virtual city environments. – *ISPRS Journal of Photogrammetry and Remote Sensing* **65**: 134–142.
- REMONDINO, F. & FRASER, C., 2006: Digital camera calibration methods: considerations and comparisons. – *The International Archives of Photogrammetry, Remote Sensing and Spatial Information Sciences* **36** (5): 266–272.
- REMONDINO, F. & RESSL, C., 2006: Overview and experiences in automated markerless image orientation. – *The International Archives of the Photogrammetry, Remote Sensing and Spatial Information Sciences* **36** (3): 248–254.
- RETSCHER, G., 2002: Accuracy Performance of Virtual Reference Station (VRS) Networks. – *Journal of Global Positioning Systems* **1** (1): 40–47.
- SABATINI, A.M., 2011: Kalman-Filter-Based Orientation Determination Using Inertial/Magnetic Sensors: Observability Analysis and Performance Evaluation. – *Sensors* **11**: 9182–9206.
- SCHWARZ, K.P. & EL-SHEIMY, N., 2004: Mobile mapping systems – state of the art and future trends. – *The International Archives of Photogrammetry, Remote Sensing and Spatial Information Sciences* **35** (B): 10 p.
- SKALOUD, J., 2006: Reliability in direct georeferencing: An overview of the current approaches and possibilities. – *EuroSDR workshop EuroCOW on Calibration and Orientation, Castelldefels, Spain*. isprs.org/commission1/euroCOW06/euroCOW06_files/papers/Eurocow06Skaloud.pdf (2011-11-08).
- TOME, P. & YALAK, O., 2008: Improvement of Orientation Estimation in Pedestrian Navigation by Compensation of Magnetic Disturbances. – *Navigation* **55** (3): 179–190.
- WACKROW, R., CHANDLER, J.H. & BRYAN, P., 2007: Geometric consistency and stability of consumer-grade digital cameras for accurate spatial measurement. – *The Photogrammetric Record* **22** (118): 121–134.
- WACKROW, R. & CHANDLER, J.H., 2008: A convergent image configuration for DEM extraction that minimises the systematic effects caused by an inaccurate lens model. – *The Photogrammetric Record* **23** (121): 6–18.
- WOODMAN, O.J., 2007: An introduction to inertial navigation. – *Computer Laboratory, University of Cambridge, Technical Report number 696*. UCAM-CL-TR-696.
- YASTIKLI, N. & JACOBSEN, K., 2002: Investigation of direct sensor orientation for DEM generation. – *The International Archives of the Photogrammetry, Remote Sensing and Spatial Information Sciences* **34** (1): 298–304.
- YASTIKLI, N. & JACOBSEN, K., 2005: Direct sensor orientation for large scale mapping – potential, problems, solutions. – *The Photogrammetric Record* **21** (111): 274–284.

Addresses of the Authors:

Asso. Prof. Dr.-Ing. DAVID HERNÁNDEZ, Universidad de Castilla-La Mancha, Departamento de Ingeniería Geológica y Minera, E-02071 Albacete, Tel.: +34-96-7599200, Fax: +34-96-7599233, e-mail: david.hernandez@uclm.es

Ing. MIRIAM CABRELLES, Universitat de València, Departamento de Prehistoria y Arqueología, E-46022 Valencia, Tel.: +34-96-3877550, Fax: +34-96-3877559, e-mail: miriam.cabrelles@uv.es

Dr.-Ing. BEATRIZ FELIPE, Universidad de Castilla-La Mancha, Instituto de Desarrollo Regional, E-02071

Albacete, Tel.: +34-96-7599200, Fax: +34-96-7599233, e-mail: beatriz.felipe@uclm.es

Asso. Prof. Dr.-Ing. JOSÉ LUIS LERMA, Universitat Politècnica de València, Department of Cartographic Engineering, Geodesy and Photogrammetry, E-46022 Valencia, Tel.: +34-96-3877550, Fax: +34-96-3877559, e-mail: jllerma@cgf.upv.es

Manuskript eingereicht: November 2011

Angenommen: März 2012